ELSEVIER

Journal of Fluids and Structures 25 (2009) 617–628

JOURNAL OF FLUIDS AND STRUCTURES

www.elsevier.com/locate/jfs

Monitoring VIV fatigue damage on marine risers

H. Mukundan*, Y. Modarres-Sadeghi, J.M. Dahl, F.S. Hover, M.S. Triantafyllou

Center for Ocean Engineering, Massachusetts Institute of Technology, 77 Massachusetts Avenue, Cambridge, MA 02139-4307, USA

Received 15 April 2008; accepted 21 March 2009
Available online 7 May 2009

Abstract

Long flexible cylinders (e.g., risers, tendons and mooring lines) exposed to the marine environment encounter ocean currents leading to vortex-induced vibration (VIV). These oscillations, often driven at high frequencies over extended periods of time, may result in structural failure of the member due to fatigue damage accumulation. Recent developments in instrumentation and installation of data acquisition systems on board marine risers have made accurate measurement of riser responses possible. This paper aims at using the data from these data acquisition devices (typically strain gages and accelerometers) in order to understand the evolution of the riser VIV, with the final aim of estimating the fatigue damage. For this purpose we employ systematic techniques to reconstruct riser VIV response using the data from the available sensors. The reconstructed riser response allows estimation of the dynamic axial stresses due to bending and consequently the estimates of the fatigue damage along the entire riser. The above methods can take into account the fatigue damage arising from complicated riser motions involving the presence of traveling waves even with the use of very few sensors. An alternate approach using a Van der Pol wake oscillator model is also explored to obtain fatigue life estimates caused by riser VIV.

Keywords: Vortex-induced vibration; Marine risers; Response reconstruction; Fatigue life estimation; Scalograms; Van der Pol wake oscillator

1. Introduction

The move to deeper waters in search of petroleum and other natural resources have resulted in the extensive use of long flexible cylindrical structures in the ocean environment. Typical examples include risers, tendons, mooring lines and pipeline spans. These flexible cylinders in the hostile marine environment need to be designed for safe operations from both a *short term* perspective and a *long term* perspective. From a short term perspective, the concerns are in maintaining the deformation, angles, working stresses, yield stresses below critical design limits. On the other hand, long term concerns include evaluating the damage of structures enduring repetitive action from the environment like corrosion and fatigue damage.

These flexible cylinders in the ocean environment encounter span-varying currents, resulting in complicated vortex shedding in their wake which depends on the flow profile; see Sarpkaya (2004). The vortex shedding results in an oscillating force on the riser leading to its vortex-induced vibration (VIV). These oscillations are driven at relatively high

*Corresponding author. Tel.: +1 857 928 2186.
E-mail address: harishm@alum.mit.edu (H. Mukundan).

0889-9746/$ - see front matter
doi:10.1016/j.jfluidstructs.2009.03.003

frequencies with amplitudes of the order of the riser diameter. Over extended periods of time, the fatigue damage due to the riser VIV accumulates and may lead to eventual failure of the structural member.

In situ monitoring of riser VIV in the marine environment has become critical. Since the loading pattern on the riser (induced by flow profile) in the ocean environment can change dramatically over the life of the riser, it is difficult to accurately predict its fatigue life before installation. In addition, recent breakthroughs in the petroleum extraction technologies have prolonged the life of several offshore fields. As a result, there is a need to use these existing offshore structures far beyond their initial design life span. In both scenarios, it is extremely important to understand the fatigue damage history of the risers and provide an estimate of the remaining life span before failure due to fatigue. There is also a concentrated effort from the regulatory bodies to ensure the health and safety of the marine installations by regular visual and automated monitoring. This is aided by the fact that significant progress has been made toward instrumenting, installation and upkeep of data-monitoring systems on marine risers. As a result, a typical riser could be instrumented using several loggers placed along its length measuring typically strains and accelerations. However, due to expensive installation, complex instrumentation and upkeep costs, only a limited number of such loggers are mounted on these risers. Thus methods for monitoring riser fatigue damage using data from a limited number of loggers are increasingly important and accessible.

The present state-of-the-art methods for monitoring VIV fatigue damage on marine risers using data from a limited number of sensors are subject to some limitations; see Trim et al. (2005) and Lie and Kaasen (2006). Some of these limitations stem from the use of riser free vibration modes, because nodal points can affect the accuracy of reconstruction; in fact the response is dominated by traveling waves, hence other basis functions provide more robust representation. Recent work by Mukundan (2008) has shown that the riser VIV response is more complicated than previously anticipated. The riser response under sheared current profiles was found to contain significant traveling wave components. Due to the complicated wake behind the riser, the effective added mass and hydrodynamic damping varies significantly. As a result, the observed riser response modes even for uniform current profile may not be pure sine-functions along the riser span. Though higher harmonics do not affect the riser VIV displacements, their noninclusion may significantly alter the riser curvatures and fatigue life estimates. Also not well understood is the well-known practice of extracting of a statistically stationary segment of the signal for fatigue life estimation. What is needed is a systematic approach to fatigue life estimation problem and a study of the factors which may affect the fatigue life estimates.

In the 1970s several researchers used the nonlinear Van der Pol equation to represent the fluctuating lift force on an elastically mounted rigid cylinder based on the similarities between observed limit cycle kind of oscillations in systems undergoing VIV and the limit cycle solutions of the Van der Pol equation; see, e.g., Billah (1989). The model succeeded in predicting the structure's behavior to some extent, but was not entirely successful in predicting the intricate details. However, a recent more successful approach was used by Violette et al. (2007) which is based on the wake oscillator model developed by Facchinetti et al. (2004). In this paper, we present a version of their wake oscillator model with the ultimate aim of obtaining the riser fatigue life estimates in a stochastic sense, by allowing model parameters to vary randomly along the length so as to capture the variability in the experimental data.

The paper is structured as follows: in the first part of this paper, we present a method to accurately obtain the dynamic stresses on a marine riser based on the response reconstruction methods developed by Mukundan (2008). The fatigue life estimation using a cycle counting algorithm is then discussed. Next, we present a method to categorize a signal (or a part of it) as *statistically stationary*. A theoretical method based on the wake oscillator model is then developed and applied to fatigue prediction. This will be followed by the use of data from high mode number experiments conducted by the Norwegian Deepwater Program (NDP) to study the effect of traveling waves, influence of higher harmonics and the use of a statistically stationary segment of the data during reconstruction for riser fatigue life estimation.

2. Reconstructing dynamic stresses on a marine riser

Consider a riser of diameter D taut between $z = 0$ and L. The instantaneous riser cross-flow (CF) displacements are denoted by $y(z, t)$. These CF displacements are measured using a finite number of sensors (loggers) placed along the length of the riser. The most important step in identifying the fatigue damage on a riser is to obtain the time varying dynamic stresses on the entire riser. The dynamic stresses $\sigma_{zz}(z, t)$ on a riser induced by bending is related to the dynamic strain $\varepsilon_{zz}(z, t)$ as $\sigma_{zz}(z, t) = E\varepsilon_{zz}(z, t)$, where E is Young's modulus of the material. The dynamic bending-induced strain (at the outermost fiber of the riser) can be estimated from the curvature of the axis of the riser $\kappa(z, t)$ as $\varepsilon_{zz}(z, t) = \frac{1}{2}D\kappa(z, t)$. Since the vortex-induced motions are of the order of a riser diameter, the curvature $\kappa(z, t)$ can be

accurately approximated by the second spatial derivative $y_{zz}(z,t)$. Thus the dynamic stresses $\sigma_{zz}(z,t)$ on a riser is related to the riser displacements as

$$\sigma_{zz}(z,t) \approx \frac{D}{2} E y_{zz}(z,t). \tag{1}$$

Thus if we have a methodology to obtain the riser displacements $y(z,t)$ along the entire riser, then we can estimate the dynamic stresses due to bending using Eq. (1) after evaluating $y_{zz}(z,t)$. However, having a sensor array which is extremely dense in space to evaluate a numerical estimate of $y_{zz}(z,t)$ is very unlikely at the present time. What we often have is a finite number of sensors (typically strain gages and accelerometers) placed along the length of the riser.

We have developed methods to reconstruct the response of the riser using the data from a limited number of sensors (loggers) placed along the length of a marine riser; see Mukundan (2008). For a scenario when a limited number of sensors are used to measure the strains and accelerations of a riser, two fundamentally different situations emerge. The available number of sensors (N_s) and the bandwidth of the measured signals allow us to classify when the measurements from the sensors contain all information pertinent to riser VIV response, and when they do not, in which case additional analytical methods are required. This classification is based on a *full reconstruction criterion* founded on the classical Nyquist's criterion ($N_s \geqslant 2N_m + 1$, where N_m is the number of spatial harmonics). The approach when we have a sensor array (large number of sensors) and the approach when we have few sensors are hence fundamentally different and are briefly described in the following sections.

2.1. Response reconstruction when large number of sensors are available

In the event when a large number of sensors are available so that the full reconstruction criterion is met, the problem of reconstructing the riser VIV response can be posed as a *spatial Fourier decomposition*. The displaced shape of the riser at any instance of time is written as a spatial Fourier series, in terms of both the sine and cosine terms. The reconstruction problem is posed as a system of linear equations, where we need to evaluate the unknown spatial Fourier coefficients at every instance of time. Since the number of sensors is larger than the critical number, we have an over-determined system of linear equations. This system is solved using a pseudo-inverse method where the least square error is minimized. This method can be applied even when a combination of acceleration, strain or displacement measurements are provided in which case, the spatial Fourier coefficients are solved in the frequency domain. This method has the advantage that it is independent of our capabilities for predicting the riser VIV response, and is applicable when the measured data is stationary or nonstationary, and for both cross-flow and in-line motion of the riser.

2.2. Response reconstruction when few number of sensors are available

The reconstruction problem of using data from few sensors arises due to expensive installation, instrumentation and upkeep costs for the on-field loggers. In this scenario, the data from the sensor measurements do not contain all information about the entire riser VIV. The reconstruction problem is posed using a *modal decomposition approach* (not to be confused with the classical mode-superposition method) where the displaced shape of the riser at any instance of time is written as a superposition of the peak response modes oscillating at the peak response frequencies. Additional information is supplied to the problem in the form of the numerically evaluated peak response modes and frequencies estimated using a prediction program like VIVA, as described in Triantafyllou (1998).

Instead of posing the reconstruction problem as a single under-determined system of equations which cannot be inverted, we use the property of separation in frequency to subdivide the system and pose it as a problem where we have several systems of equations each of which are well behaved. The detailed approach is mentioned in Mukundan (2008). Since we need to input the data in the form of peak response mode and peak response frequencies, the accuracy of the method depends on the predictive capabilities which require the estimation of the steady flow profile. The accuracy of predicting the riser VIV motions can be improved by using a data assimilation approach where the data from the few sensors are used to re-calibrate the lift coefficient databases thereby improving the predictions and the resulting reconstruction.

An underlying assumption while using a mode-based prediction program is that of a steady state response (a steady flow profile leading to a steady response). One characteristic of a riser under a steady state response is that the measurements from such a riser would be *statistically stationary*. Because of this, it is a common practice to extract a statistically stationary segment of the measured data for performing reconstruction and fatigue life estimation. The justification for the use of a statistically stationary part of the measured data will be presented at a later stage in this paper.

3. Fatigue damage estimation method

The reconstruction methods described in Sections 2.1 and 2.2 allow us to produce the displacement signal at any location along the riser using signals from a limited number of sensors. In this work our focus will be on reconstructing the riser cross-flow motions and the associated fatigue life estimates. The dynamic bending induced axial stresses $\sigma_{zz}(z,t)$ are obtained from the reconstructed riser displacements using the relation given in Eq. (1).

Once we obtain the dynamic stresses $\sigma_{zz}(z,t)$, we can estimate the fatigue damage using Miner's rule, which allows us to add the damages due to each cycle of stress. For more detail refer to Lee et al. (2005). Miner's rule requires the estimation of the number of stress cycles corresponding to each stress range in the signal. Corresponding to an input stress signal $\sigma(t)$ of length of time T, the number of stress cycles n_i and the corresponding stress range σ_i may be obtained using a cycle counting method like the *rainflow algorithm*. The rainflow method first identifies the turning points on the stress signal (corresponding to local maxima and minima). The difference between the consecutive turning points gives the stress range σ_i and corresponds to one half cycle. We count the number of half-cycles for each of the stress range over the length of the signal. The end result is a histogram which tabulates the number of stress cycles n_i corresponding to various stress ranges σ_i. Using Miner's rule, the maximum number of stress cycles (N_i) the material can endure before failure corresponding to a stress range σ_i is obtained from the $S-N$ curve of the material. The fatigue damage rate D_r due to the n_i stress cycles with a stress magnitude σ_i over the length of time T is obtained as

$$D_r = \frac{1}{T}\sum_i \frac{n_i}{N_i}. \tag{2}$$

The fatigue life T_{fatigue} assuming a damage rate D_r is obtained as $T_{\text{fatigue}} = 1/D_r$. An $S-N$ curve of the form $N_i = A\sigma_i^{-B}$ is often recommended and used. Reconstruction allows us to obtain the stress signals at any location along the riser. As a result, we can obtain the fatigue life estimate along the entire riser $T_{\text{fatigue}}(z)$. The overall algorithm for estimating the riser fatigue life is illustrated in the flowchart given in Fig. 1.

4. Extracting statistically stationary regions of measured data using scalograms

As mentioned in Section 2, reconstruction methods involving Fourier decomposition which require a large number of sensors are independent of prediction schemes. However, the reconstruction methods employing prediction schemes (methods using modal decomposition) require us to present segments of the measured data which are statistically stationary. In this section we illustrate the use of scalograms for extracting statistically stationary segments of the VIV measurements.

A plot of the measured signal against time (Fig. 2(a)) gives limited information on the evolution of a process; a plot of its finite-window spectrum (Fig. 2(b)) can give much better information on the frequency content of the process, but presents difficulties when the frequency content of the signal changes with time. However, employing time evolution plots (*scalograms*) (Fig. 2(c)) offers far more insight into the evolution of the physical process. A scalogram is a contour plot of squared magnitude of a continuous wavelet transform which describes how the frequency content of a signal varies with time; refer to Boashash (2003). From a VIV perspective, a scalogram can be used to: (a) obtain a snapshot of

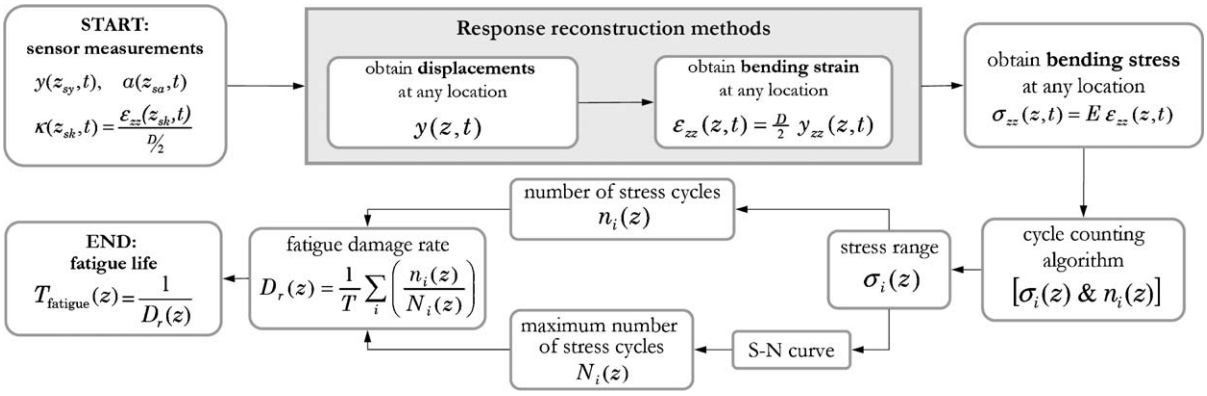

Fig. 1. Overview of the proposed algorithm for estimating the fatigue life of a riser based on data from limited number of displacement-based sensors (strain gages and accelerometers).

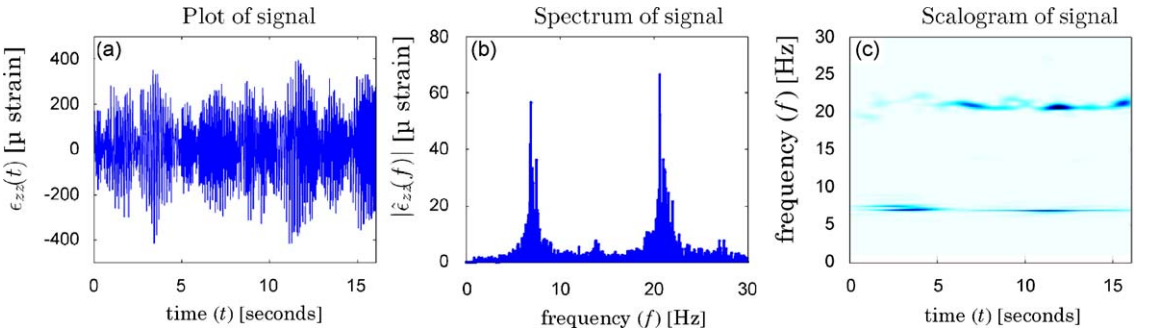

Fig. 2. Three different representations of the CF strain signal measured at $z = 8.61$ m for NDP dataset 2110. (a) A plot of the time signal; (b) the spectrum of the signal; (c) the scalogram of the signal.

the evolution of the underlying physical phenomenon; (b) eliminate faulty data arising from instrumentation errors or processing errors as a result of the very complicated instrumentation of a riser during field experiments; (c) isolate a region over which the process is statistically stationary.

The present state-of-the-art analysis of riser VIV assumes a steady state excitation and any benchmark study will require the benchmarking signal to be statistically stationary. A statistically stationary signal has all its statistical moments independent of time. For a vibrating riser this implies that the fluid excitation is also statistically stationary. For a stationary signal, the energy content corresponding to each frequency in the signal remains constant. It is easier and meaningful to relax this criterion to categorize the VIV motions as second-order stationary (SOS), if the statistics such as the standard deviation and autocorrelation function (relevant to the frequency content) remain nearly constant, within a reasonable threshold. We identify segments over which the response is second-order stationary.

As shown using example in Fig. 2(c), the regions of high intensity in the contour plot correspond to the dominant frequencies which are excited over time. A statistically stationary signal results in scalograms containing horizontal lines of constant intensity, implying that the energy distribution remains constant along those frequencies. In Fig. 2(c), the sharp horizontal streaks (e.g. between $t = 12.5$ s and $t = 15$ s) depict two narrow banded peak frequencies which are excited more than the others. The parallel lines of lesser intensity depict the other frequencies which are also excited. Fig. 2(c) depicts a nonstationary signal between $t = 0$ and 5 s where the dominating frequencies change over time. Even though the whole signal may not be considered as stationary, we may identify segments of the time series over which the signal is considered to be stationary. We extracted statistically stationary segments of the response from a visual inspection of the scalograms.

5. Van der Pol wake oscillator model with random parameters

In an attempt to model the riser VIV and predict the resultant fatigue life we utilize a method based on the Van der Pol wake oscillator model with random parameters. In the classic Van der Pol model, the dynamics of the rigid cylinder is described using a linear forced oscillator model, in which the external force (external to the rigid cylinder) comes from the wake and the wake itself is described by a forced Van der Pol oscillator equation. The external force acting on the Van der Pol wake oscillator is related to the cylinder oscillation by a coupling term proportional to the cylinder's displacement, velocity or acceleration. Facchinetti et al. (2004) investigated various possible coupling terms and concluded that a coupling term proportional to the acceleration gives the best results. Violette et al. (2007) extended this Van der Pol wake oscillator model to the case of a long flexible structure. In their model, the structure is described by a simple linear beam equation, where the forcing term coming from the wake exists on the right-hand side of the equation. The excitation from the wake is described using a Van der Pol equation whose forcing term is proportional to the structure's acceleration. Their model, in mathematical form, reads as

$$\frac{\partial^2 y}{\partial t^2} + \frac{\gamma\omega_f}{\mu}\frac{\partial y}{\partial t} - c^2\frac{\partial^2 y}{\partial z^2} + b^2\frac{\partial^4 y}{\partial z^4} = \omega_f^2 M q, \quad \frac{\partial^2 q}{\partial t^2} + \varepsilon\omega_f(q^2 - 1)\frac{\partial q}{\partial t} + \omega_f^2 q = A\frac{\partial^2 y}{\partial t^2}, \tag{3}$$

where $\gamma = C_D/4\pi\mathrm{St}$ is the stall coefficient, $\omega_f = \Omega_{\mathrm{Ref}}(z)/\Omega_{\mathrm{Ref}} = U_{\mathrm{Ref}}(z)/U_{\mathrm{Ref}}$ is the nondimensional shedding frequency, $\mu = (m_{\mathrm{cyl}} + m_{\mathrm{fluid}})/\rho D^2$ mass ratio, $c^2 = [K/(m_{\mathrm{cyl}} + m_{\mathrm{fluid}})]/(\Omega_{\mathrm{Ref}} D)^2$ nondimensional tension, $b^2 = [EI/(m_{\mathrm{cyl}} + m_{\mathrm{fluid}})]/(\Omega_{\mathrm{Ref}} D^2)^2$ nondimensional bending stiffness, $M = C_{L0}/(2\,8\pi^2\mathrm{St}^2\mu)$ is a coefficient of the forcing term acting on the structure due to the wake dynamics, and A and ε are the coefficients in Van der Pol equation. In the

above relations, D is the diameter, C_D the drag coefficient, St the Strouhal number, C_{L0} the fluctuating lift coefficient, Ω_{Ref} the reference frequency, U_{Ref} the reference velocity, K the tension, EI the flexural rigidity, m_{cyl} the mass per unit length of the cylinder and m_{fluid} the mass per unit length of the fluid.

In a Van der Pol wake oscillator model it is usually assumed that the Van der Pol coefficients (ε, A), fluctuating lift coefficient (C_{L0}) and drag coefficient (C_D) are constant parameters. In the model used in this paper, the traditionally constant parameters are assumed to be randomly varying along the length in an effort to take into account the strong randomness observed in the available experimental data. Facchinetti et al. (2004) suggested the mean values of 0.3 and 12 for ε and A, based on a best fit to a series of experimental results, which implies these values can be treated as random numbers to account for the variation in experimental results used in the curve-fitting. Also, assuming constant values for C_{L0} and C_D is not a wise decision, especially when large variations in frequency and amplitude of oscillations are observed along the length, as these parameters depend on both frequency and amplitude of oscillations, which are not known *a priori*. By assuming random C_{L0} and C_D, we account for this variation to some extent. The random parameters therefore are

$$\varepsilon(\zeta) = \varepsilon_m\left[1+\sigma_\zeta\left(\xi_\zeta+\sum_{i=1}^{N} g_i(\zeta,\xi)\right)\right], \quad A(\zeta) = A_m\left[1+\sigma_\zeta\left(\xi_\zeta+\sum_{i=1}^{N} g_i(\zeta,\xi)\right)\right], \tag{4}$$

$$C_L(\zeta) = C_{L0_m}\left[1+\sigma_\zeta\left(\xi_\zeta+\sum_{i=1}^{N} g_i(\zeta,\xi)\right)\right], \quad C_D(\zeta) = C_{D_m}\left[1+\sigma_\zeta\left(\xi_\zeta+\sum_{i=1}^{N} g_i(\zeta,\xi)\right)\right], \tag{5}$$

where $\zeta = z/L$, z is the position along the length of the riser, ξ is a random number, $\varepsilon_m, A_m, C_{L0_m}$ and C_{D_m} are mean values, σ_ζ is standard deviation and g is a continuous function with a random peak along the length. One of the strengths of this model is that it has only a few (four) random parameters, and its main advantage in comparison with direct numerical simulation methods is its low computational cost, which makes it suitable for parametrical as well as statistical studies.

6. Norwegian Deepwater Programme high mode VIV tests

The experimental data used in this paper are from high mode VIV experiments sponsored by the Norwegian Deepwater Programme discussed in more detail by Trim et al. (2005) and Braaten and Lie (2004). A 38 m long riser model made of fiber glass with diameter 0.027 m, linear mass density in air 0.761 kg m^{-1}, Young's modulus 2.25×10^9 N m^{-2} under a tension 4000–6000 N was used for the test runs. The riser model was taut horizontally and towed at different speeds, simulating uniform and triangular shear currents. Uniform flow profile is achieved by towing both ends of the riser simultaneously at the same velocity. For a triangular sheared flow profile, one end of the riser was kept at rest while the other end was made to follow a predefined circular arc. The riser was instrumented with strain gages and accelerometers to record both in-line and cross-flow bending strains and accelerations along the riser. The maximum number of strain gages in CF direction was 24 and in the IL direction was 40. There were eight biaxial accelerometers recording accelerations in CF and IL directions.

7. Results from application of methods to NDP datasets

To illustrate the fatigue damage estimation methodology, we consider triangular current profile cases in the NDP datasets of the form $U(z) = U_{\max}(1-z/L)$. The fatigue damage estimation uses an $S-N$ curve with parameters $A = 4.8641\times10^{11}$ and $B = 3$ obtained from the NORSOK (1998) standards.

The large number of sensors (24 strain gages and 8 accelerometers) satisfies the full reconstruction criterion for a variety of datasets. Since the Fourier decomposition method gives a reconstruction independent of prediction, we prefer this method unless we have a scenario where data from very few sensors are available to us, in which case a modal decomposition approach may be used. The reconstruction method mentioned in Section 2.1 can be applied to accurately obtain the riser displacements continuously at every location along the riser. The reconstruction of riser curvature $\kappa(z,t)$ by taking the numerical spatial derivatives (finite difference) is not the ideal method. We chose to obtain the curvatures by writing it as a spatial Fourier series given by $\kappa(z,t) = \sum(n\pi/L)^2 \times [a_n(t)\cos(n\pi(z/L)+ b_n(t)\sin(n\pi(z/L))]$, where we already know the time varying spatial Fourier coefficients $a_n(t)$ and $b_n(t)$ which were solved while reconstructing the riser displacements. The use of this technique also results in significant savings in the computational time during the curvature evaluation. As noted previously, unless specifically mentioned we prefer to use a statistically stationary segment of the measurement for the reconstruction.

The results from the reconstruction method is observed as plots depicting the rms of the riser displacements, curvatures, bending induced stresses and finally the fatigue life estimates along the length of the riser (refer to Figs. 3–6). The reconstructed quantity is plotted as a continuous curve and the data from the sensors (unprocessed data and data after preprocessing) are plotted as data points along the riser. Observation of the reconstruction (displacements, curvatures, stresses and fatigue life) clearly show that these quantities closely match the preprocessed data which is input to the reconstruction algorithm at the sensor locations. Another interesting observation is the fact that with increasing flow velocity, the fatigue life estimate progressively decreases. In the following section, we study the influence of some of the underlying assumptions during the use of the reconstruction algorithm for fatigue life estimation.

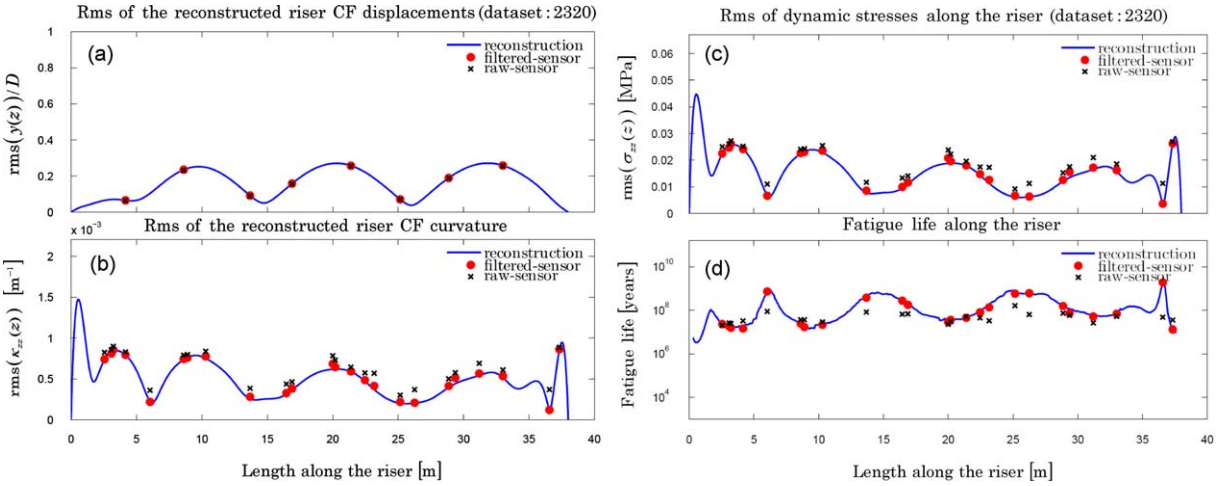

Fig. 3. Results from the application of the fatigue damage reconstruction method applied to NDP dataset 2320 ($U_{max} = 0.4\,m\,s^{-1}$). (a) The rms of the reconstructed displacement and the displacement at the accelerometer locations; (b) rms of the reconstructed CF curvature and the curvatures obtained from the strain gages; (c) rms of the reconstructed and strain gage measured dynamic stresses showing a stress hotspot near the end of the riser which encounter higher flow velocities; (d) fatigue life estimates along the riser after reconstruction matches the fatigue life at chosen sensor locations.

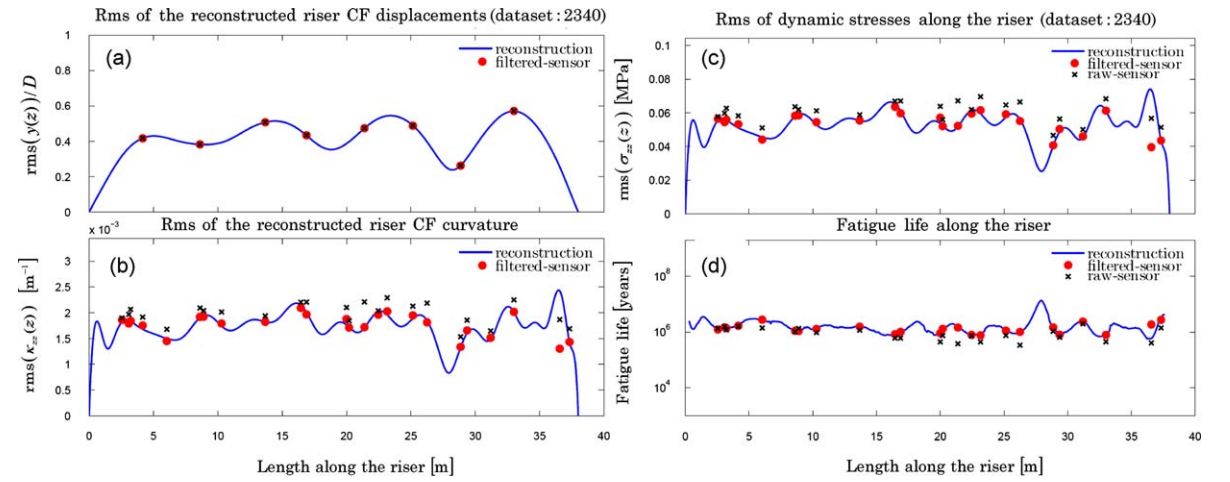

Fig. 4. Results from the application of the fatigue damage reconstruction method applied to NDP dataset 2340 ($U_{max} = 0.6\,m\,s^{-1}$). (a) The rms of the reconstructed displacement and the displacement at the accelerometer locations; (b) rms of the reconstructed CF curvature and the curvatures obtained from the strain gages; (c) rms of the reconstructed and strain gage measured dynamic stresses showing a stress hotspot near the end of the riser which encounter higher flow velocities; (d) fatigue life estimates along the riser after reconstruction matches the fatigue life at chosen sensor locations.

7.1. Influence of traveling waves on fatigue life estimates

The authors have previously shown the importance of traveling wave behavior in the VIV response of a riser especially under sheared flow profiles; see Mukundan (2008). Both the reconstruction methods (for large number of sensors and few number of sensors) allow reconstruction of both the traveling wave and standing wave behavior of the riser VIV response. In the case of large number of sensors, this is aided by the use of both cosine and sine terms during

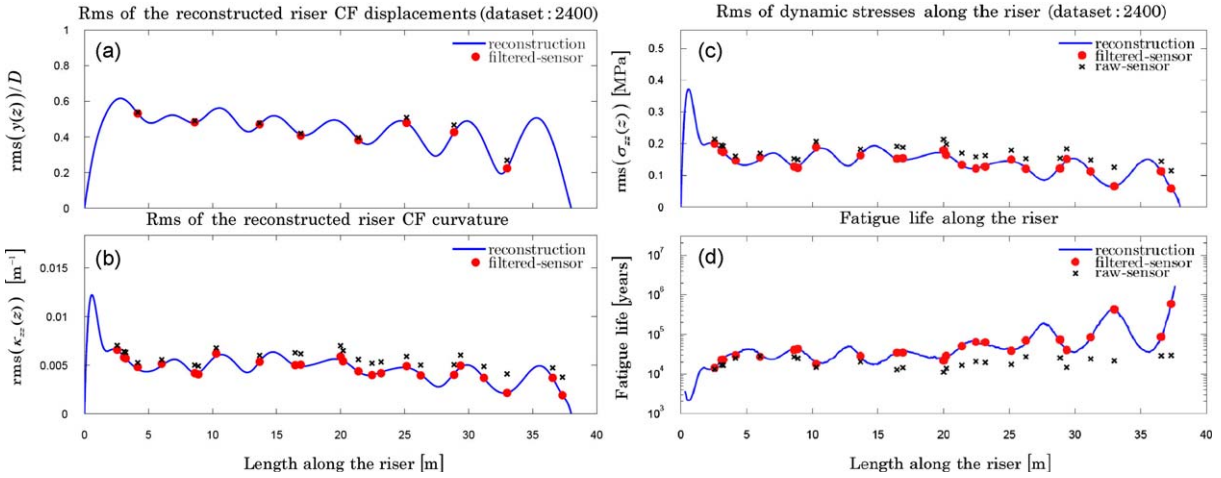

Fig. 5. Results from the application of the fatigue damage reconstruction method applied to NDP dataset 2400 ($U_{max} = 1.2\,m\,s^{-1}$). (a) The rms of the reconstructed displacement and the displacement at the accelerometer locations; (b) rms of the reconstructed CF curvature and the curvatures obtained from the strain gages; (c) rms of the reconstructed and strain gage measured dynamic stresses showing a stress hotspot near the end of the riser which encounter higher flow velocities; (d) fatigue life estimates along the riser after reconstruction do not match the fatigue life at chosen sensor locations, because we did not include the higher harmonic components during reconstruction.

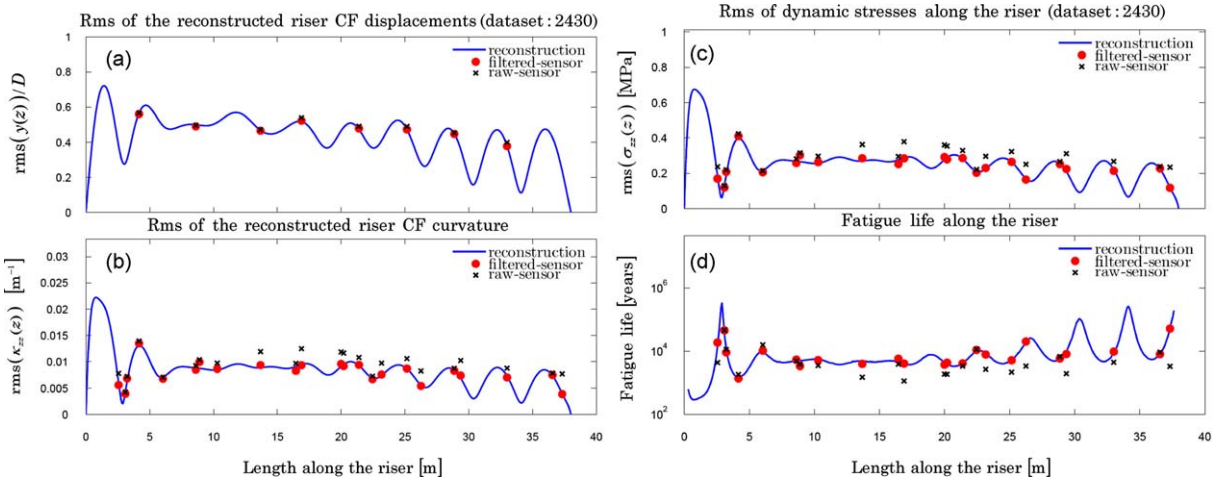

Fig. 6. Results from the application of the fatigue damage reconstruction method applied to NDP dataset 2430 ($U_{max} = 1.5\,m\,s^{-1}$). (a) The rms of the reconstructed displacement and the displacement at the accelerometer locations; (b) rms of the reconstructed CF curvature and the curvatures obtained from the strain gages; (c) rms of the reconstructed and strain gage measured dynamic stresses showing a stress hotspot near the end of the riser which encounter higher flow velocities; (d) fatigue life estimates along the riser after reconstruction do not match the fatigue life at chosen sensor locations, because we did not include the higher harmonic components during reconstruction.

reconstruction. On the other hand, for the case of few sensors, the use of modal decomposition involving the complex peak response modes allows the reconstruction of both standing and traveling wave behavior.

From Figs. 3–6, we observe that even though the displacements are well within the range of riser diameter, the stresses are more complicated. The presence of traveling waves tend to affect the dynamic stresses (curvatures) on the ends of a marine riser. The fatigue life estimates are shown to be up to an order of magnitude smaller near the boundary resulting in fatigue damage hotspots especially near the ends of the riser closer to the high flow velocity regions. The previous methods mentioned in Trim et al. (2005) and Lie and Kaasen (2006) may or may not consider the presence of traveling waves during reconstruction and the resultant increase in the dynamic stress hotspots near the riser ends. This is especially true with other methods which may utilize data from very few sensor measurements because of their use of free vibration modes which are real functions and hence cannot accommodate span-wise phase variation.

7.2. Influence of higher harmonics on fatigue life estimates

The NDP datasets contain data from 24 strain gages and 8 accelerometers (32 in total). As a result, three scenarios emerge: (i) both harmonic and higher harmonic components can be reconstructed using Fourier decomposition method; (ii) only harmonic component of the riser response can be obtained using Fourier decomposition method; (iii) only harmonic component of the riser response can be obtained using a modal decomposition method. Reconstructing the higher harmonic components using the modal decomposition method requires a model to predict the peak response modes corresponding to the higher harmonic components in the riser response.

Since the higher harmonic terms produce negligible effect on the riser displacements, we perform a preprocessing step where the higher harmonic terms are removed by filtering, so that there is no pathological effect of spatial aliasing [refer to Mukundan (2008)]. We investigate the effect of the preprocessing step of removing the higher harmonics before reconstruction. For this purpose two low flow velocity cases where we anticipate to reconstruct the higher harmonics and two high flow velocity cases where the higher harmonics needed to be removed are studied in detail.

For the lower velocity cases considered, i.e. dataset 2320 ($U_{\max} = 0.4\,\mathrm{m\,s^{-1}}$) and dataset 2340 ($U_{\max} = 0.6\,\mathrm{m\,s^{-1}}$), the fatigue life estimates from the original raw strain measurements closely match the fatigue life estimates from reconstruction as illustrated in Figs. 3(d) and 4(d). On the other hand, for higher flow velocity cases dataset 2400 ($U_{\max} = 1.2\,\mathrm{m\,s^{-1}}$) as illustrated in Fig. 5(d) and dataset 2430 as illustrated in Fig. 6(d) ($U_{\max} = 1.5\,\mathrm{m\,s^{-1}}$), there is at least one order of magnitude deviation between the reconstructed fatigue life estimate and the estimates observed from the raw unfiltered strain gage measurements at the sensor locations. Here the reported fatigue life estimates are very large (order of magnitude 10^3 to 10^7 years), although the magnitude change in fatigue life would be much more important for structures which are designed with an estimated fatigue life of the order of 10^3 years. Not considering the higher harmonic components has the effect of underestimating the fatigue damage rates (or overestimating the fatigue life estimates) by orders of magnitude. This pathological scenario needs to be overcome to obtain accurate fatigue damage estimates on marine risers. Improved fatigue damage estimates may be obtained by being able to accurately model the peak response modes corresponding to the higher harmonics on the riser. Though extensive research on the higher harmonic forces are presented by Dahl (2008), such a capability is well beyond the present available knowledge of the VIV community.

7.3. Influence of statistically stationary segments in riser response on fatigue life estimates

For each dataset from the NDP experiment, we obtain the scalograms for each strain gage measurements from which we obtain a statistically stationary segment of the sensor measurements. The scalograms illustrate that significant portions of the signals from the NDP datasets can be considered as statistically stationary. Two examples are illustrated as follows:

Example I (*NDP dataset* 2400). Fig. 7(a) and (b) depict the scalograms of the strain signal obtained at 2 representative locations along the riser for the NDP dataset 2400. Based on the observations from the scalograms obtained at all the strain gage locations, we choose a segment from 12.5 to 16.5 s as our choice of a statistically stationary segment of data.

Example II (*NDP dataset* 2410). In a similar fashion, Fig. 7(c) and (d) depicts the scalograms of the strain signal obtained at 2 representative locations along the riser for the NDP dataset 2410. Again we choose a statistically stationary region of the signal based on a visual observation of the scalograms obtained for all the strain signals. Our choice is from 25.5 s to 29 s.

The fatigue life estimates are obtained from strain measurements at the strain gage locations for various triangular shear flow datasets corresponding to three separate scenarios of (a) entire signal, (b) statistically stationary segment of the signal, and (c) nonstationary part of the signal. Fig. 8 depicts the minimum value (Fig. 8(a)), the mean value

(Fig. 8(b)) and the root mean square value (Fig. 8(c)) of the fatigue life estimate $T_{\text{fatigue}}(z)$ taken over each of the strain gages for the three separate parts of the signals. Fig. 8(a) illustrates that over a range of flow velocities, the fatigue life estimates from a stationary segment of the measurements yield a more conservative estimate than that based on the entire signal, or the nonstationary part of the signal. However, the use of a stationary segment may overestimate the other metrics like the rms and the mean value of the fatigue life along the entire riser. Fig. 8(a) also shows that the fatigue life estimates decrease in an exponential fashion as the maximum flow velocity $U_{\max}$ increases.

We can also obtain the fatigue life estimates based on segmenting the original measured signal into several pieces, reconstruct each subsegment and obtain fatigue life estimate based on each segment. Fatigue life based on each such segment of the measured data gives a completely different estimate. This variability in the fatigue life estimate is captured by the variance $\sigma^2(z)$ obtained by evaluating the various fatigue life estimates using each subsegment of the measured data. The standard deviation $\sigma(z)$ is obtained as

$$\sigma(z) = \mathbb{S}\{T_{\text{fatigue}_1}(z), \quad T_{\text{fatigue}_2}(z), \quad T_{\text{fatigue}_3}(z), \ldots, \quad T_{\text{fatigue}_i}(z), \ldots\}, \tag{6}$$

where $T_{\text{fatigue}_i}(z)$ represents the fatigue life estimate based on the ith segment of the measured data, and $\mathbb{S}\{\}$ represents the standard deviation operator. One can also obtain a mean value of the fatigue life estimate $\bar{T}_{\text{fatigue}}(z)$ from the above ensemble.

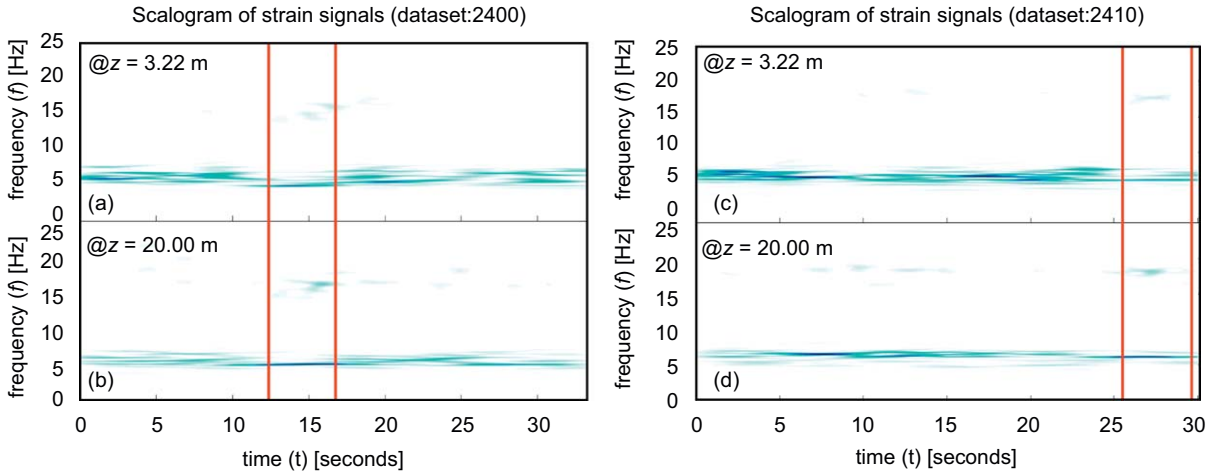

Fig. 7. Scalograms of strain signals obtained at 2 representative locations along the riser for NDP dataset 2400 ($U_{\max} = 1.2\,\text{m s}^{-1}$), and our choice of the statistically stationary segment of data ($t_{\text{stationary}} = [12.5, 16.5]$ s) shown between the two vertical lines ((a) and (b)). Scalograms of strain signals obtained at 2 representative locations along the riser for NDP dataset 2410 ($U_{\max} = 1.3\,\text{m s}^{-1}$), and our choice of the statistically stationary segment of data ($t_{\text{stationary}} = [25.5, 29]$ s) shown between the two vertical lines ((c) and (d)).

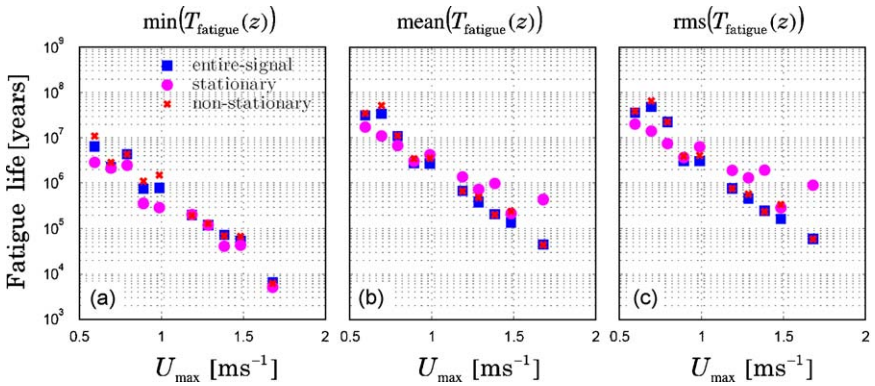

Fig. 8. (a) The minimum, (b) mean and (c) root mean square of the fatigue life estimates $T_{\text{fatigue}}(z)$ over the length of the riser (from the strain gages) for various triangular shear flow profiles with maximum flow velocity $U_{\max}$ corresponding to the entire-signal, a statistically stationary part of the signal and the nonstationary part of the signal.

The above method is employed to obtain a fatigue life error bound $\bar{T}_{\text{fatigue}}(z) \pm \sigma(z)$ on the NDP datasets. In practice we divide the signal into various segments each of which is 5 s long. The mean estimate $\bar{T}_{\text{fatigue}}(z)$ and the error bounds for various NDP datasets are produced in Fig. 9. We can observe that at low flow velocity datasets, the error bounds more or less contains all the fatigue life evaluated at the sensor locations. As the flow velocity increases, there is an overestimation of the fatigue life estimates primarily due to the presence of higher harmonic components which are not captured at high flow velocity cases during reconstruction.

7.4. Fatigue life estimates from the wake oscillator model and comparison with experimental results

Our choice of parameters for the theoretical model is as follows: $\varepsilon_m = 0.3$, $A_m = 12$, $C_{L0_m} = 0.3$, $C_{D_m} = 0.1$ and $\text{St} = 0.17$. The values for ε_m and A_m were suggested by Facchinetti et al. (2004). The mainly traveling-wave behavior observed in the experimental case is reproduced here (similar to the experimental case, motion close to the boundaries is mainly a standing wave). The response amplitude (varying from $-0.8D$ to $0.8D$) and the frequency of oscillations ($f \approx 8$ Hz) are very similar to those observed experimentally for dataset 2430 ($U_{\max} = 1.5\,\text{m s}^{-1}$). Fatigue estimates can be obtained for every theoretical run and the statistics of the results are compared with that from the experiments in Fig. 10. Though the fatigue life estimates from the theoretical model vary significantly over each choice of random

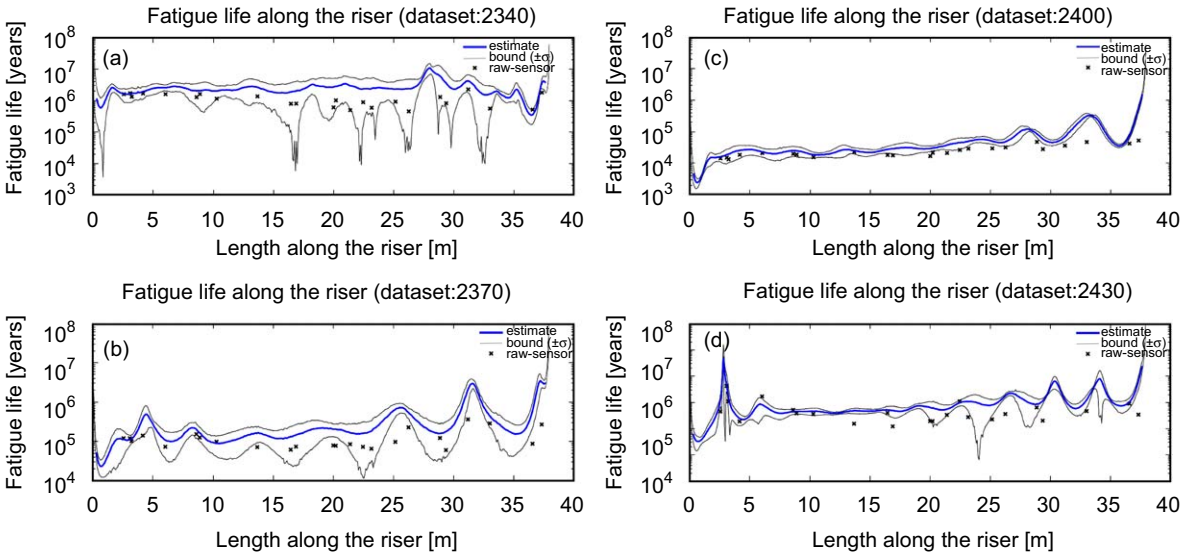

Fig. 9. Fatigue life estimates along the riser length, $T_{\text{fatigue}}(z)$. Blue color line denotes mean value, gray color lines denote bounds one standard deviation from mean: (a) NDP dataset 2340 ($U_{\max} = 0.6\,\text{m s}^{-1}$); (b) NDP dataset 2370 ($U_{\max} = 0.9\,\text{m s}^{-1}$); (c) NDP dataset 2400 ($U_{\max} = 1.2\,\text{m s}^{-1}$); (d) NDP dataset 2430 ($U_{\max} = 1.5\,\text{m s}^{-1}$). (See web version of the article for color reference).

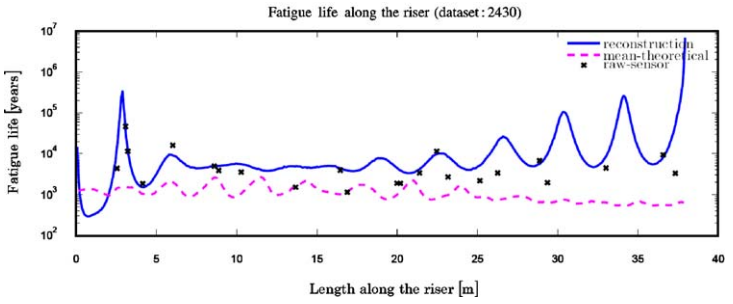

Fig. 10. A comparison of reconstructed fatigue life estimates along the entire riser, the mean value of the fatigue life from various runs of the Van der Pol model, and the fatigue life estimates corresponding to raw sensor measurements. The theoretical model developed captures the minimum fatigue life from the raw experimental data fairly well, although the reconstruction method estimates a lower fatigue life.

parameters, the mean value of the fatigue life obtained over the ensemble for the example dataset was found to be very relevant. Fig. 10 shows this trend where the minimum value of the fatigue life measured in the field compares very well with the mean value of the fatigue life from theoretical estimates.

8. Conclusions

The problem of reconstructing the vortex-induced response and the associated estimation of the fatigue life on a marine riser based on the data from a limited number of sensors placed along the length is increasingly important. In this paper, we have developed a fatigue damage estimation method based on our state-of-the-art response reconstruction methods and have applied the method to several datasets from the NDP experiments. Various assumptions made during the formulation of the reconstruction problem were dissected and their influence on the fatigue life estimation was discussed.

Our analysis shows that the traveling wave characteristics of riser VIV response are captured by the reconstruction methodologies. On the other hand, the effect of higher harmonic components were found to influence the riser fatigue life, and may or may not be captured by the method depending on the available number of sensors and the bandwidth of the observed VIV response. In fact, to capture the effect of the third harmonic components, we may need data from three times the minimum number of sensors required if we were interested in only the harmonic components; or an appropriate theoretical model which will predict the higher harmonic riser response modes is required. Based on the data corresponding to a set of triangular flow profiles, we observe that the minimum fatigue life estimated using a stationary part of the signal is sufficient, and provides a conservative estimate of the fatigue life. The stochastic approach developed using a Van der Pol oscillator model with random parameters was found to produce a rough estimate of the minimum fatigue life along the riser.

Acknowledgments

The authors gratefully acknowledge the financial support from the MIT-BP Major Projects Program, monitored by Neil Kitney and Pierre Beynet; as well as the generous permission by the Norwegian Deepwater Programme, provided through Dr Kjetil Skaugset, to use the experimental data on a 38 m riser model. The second author acknowledges with gratitude the financial support given to him from Le Fonds Québécois de la Recherche sur la Nature et les Technologies (FQRNT).

References

Billah, K.Y.R., 1989. A study of vortex-induced vibrations. Ph.D. Thesis, Princeton University, Princeton, NJ, USA.

Boashash, B. (Ed.), 2003. Time Frequency Signal Analysis and Processing: A Comprehensive Reference, 1st ed. Elsevier, Oxford, UK.

Braaten, H., Lie, H., 2004. NDP riser high mode VIV tests main report. Main report number 512394.00.01, Norwegian Marine Technology Research Institute.

Dahl, J.M., 2008. Vortex induced vibrations of a circular cylinder with combined in-line and cross-flow motions. Ph.D. Thesis, Massachusetts Institute of Technology, Cambridge, MA, USA.

Facchinetti, M.L., de Langre, E., Biolley, F., 2004. Coupling of structure and wake oscillators in vortex-induced vibrations. Journal of Fluids and Structures 19, 123–140.

Lee, Y.L., Pan, J., Hathaway, R., Barkey, M. (Eds.), 2005. Fatigue Testing and Analysis: Theory and Practice. Elsevier, Amsterdam.

Lie, H., Kaasen, K.E., 2006. Modal analysis of measurements from a large-scale VIV model test of a riser in linearly sheared flow. Journal of Fluids and Structures 22, 557–575.

Mukundan, H., 2008. Vortex-induced vibration of marine risers: motion and force reconstruction from field and experimental data. Ph.D. Thesis, Massachusetts Institute of Technology, Cambridge, MA, USA.

NORSOK, 1998. Design of steel structures, annexure-C: fatigue strength analysis.

Sarpkaya, T., 2004. A critical review of the intrinsic nature of vortex-induced vibrations. Journal of Fluids and Structures 19, 389–447.

Triantafyllou, G.S., 1998. Vortex induced vibrations of long cylindrical structures. In: Proceedings of 1998 ASME Fluids Engineering Division Summer Meeting (FEDSM98). Washington, DC.

Trim, A.D., Braaten, H., Lie, H., Tognarelli, M.A., 2005. Experimental investigation of vortex-induced vibration of long marine risers. Journal of Fluids and Structures 21, 335–361.

Violette, R., de Langre, E., Szydlowski, J., 2007. Computation of vortex-induced vibrations of long structures using a wake oscillator model: comparison with DNS and experiments. Computers and Structures 85, 1134–1141.